

# FATIGUE CRACK GROWTH SIMULATION FOR COMPLEX THREE-DIMENSIONAL GEOMETRY AND LOADING

Thomas J. Curtin, Robert A. Adey, John M.W. Baynham, Philip Marais  
Computational Mechanics Inc.  
Billerica, Massachusetts, 01821, USA  
978-667-5841  
978-667-7582  
[cmina@ix.netcom.com](mailto:cmina@ix.netcom.com)

## ABSTRACT

The focus of this paper is on the implementation of the boundary element method to investigate the impact of cracks in aerospace components. The theoretical background of the boundary element based fracture mechanics algorithms is discussed and the capability of the method is illustrated with applications pertinent to the aerospace industry. The methodology and applications discussed in this paper are based on the BEASY Fatigue and Crack Growth software developed by Computational Mechanics Inc. The boundary element method utilized in the software is well suited for simulating fracture and crack propagation. The BEASY fracture simulation tool can be easily incorporated in damage tolerance programs and serve to provide quantitative data in terms of the impact of fracture related damage.

## 1. INTRODUCTION

The high priority given to aging aircraft evaluation has resulted in a critical need for accurate and easy to use crack simulation software in the aerospace industry. Both military and commercial aircraft are aging and procurement of new aircraft is often restricted by budget limitations. Inventory assessment in the aircraft industry conducted during the early 1990s revealed that approximately 45 percent of the U.S. military and commercial aircraft fleet are over 15 years old. As a result of this aging fleet, airframe damage tolerance programs have been spawned to help predict residual life of aircraft and assess their continued airworthiness.

For damage tolerance program to be effective it is essential that fracture data can be evaluated in a quantitative manner. Fracture mechanics software provides the engineering community with this capability. Computer codes can be used to predict fatigue crack growth and residual strength in airframe structures. They can also be useful to determine in-service inspection intervals, time-to-onset of widespread fatigue damage and to design and certify structural repairs. Used in conjunction with damage tolerance programs fracture analysis codes can play an important role in extending the life of "high-time" aircraft.

## 2.0 FRACTURE MECHANICS USING THE BOUNDARY ELEMENT METHOD

### 2.1 Dual Boundary Element Method

The dual boundary element method is well suited to handle analysis of general embedded cracks and edge crack problems. The DBEM crack modeling strategy forms the basis of the dual

boundary element technology incorporated in the BEASY analysis algorithms. The dual boundary element method (DBEM) considers two independent equations, the displacement and traction boundary integral equations, within the same integration path for each pair of coincident source points [1, 10]. This crack modeling strategy allows a single-region boundary element analysis of a cracked body. The crack is represented by two elements occupying the same physical location, each element representing a face of the crack. The displacement and traction boundary integral equations are applied on the crack surfaces.

Because of the continuity requirements of the displacements and tractions for the existence of the traction BIE and the coplanar characteristics of crack surfaces, special consideration has to be taken for the discretization in the modeling. The introduction of discontinuous elements fulfils this continuity requirement for boundary variables while edge discontinuous elements give a necessary smooth transition from continuous to discontinuous elements on the boundary [2, 3].

## 2.2 Discontinuous Elements

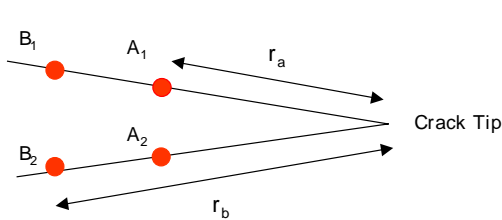
Discontinuous elements play an important role in the boundary element method because the problem variables are not forced to be continuous across elements. The major benefit of discontinuous elements is their ability to model discontinuous stress results. They are therefore very useful in fracture mechanics analysis for modeling the stress behavior at a crack front.

A discontinuous element is represented as an element where the mesh point and node locations are not coincident. As a result of this formulation the nodes are not shared between elements. The geometry of the element is approximated by the mesh point location and shape functions. The variation of the traction and displacement boundary variables within the element is represented by values at the node location and interpolation functions [3].

## 2.3 Stress Intensity Factor Solution

In general the geometry and loading encountered in three-dimensional crack problems is too complex for the stress intensity factor (SIF) to be solved analytically. The SIF calculation is further complicated because it is a function of the position along the crack front, crack size and shape, type of loading, and the geometry of the structure.

Three-dimensional SIF solutions can be computed using a displacement extrapolation technique that involves correlation of the boundary element displacements on the crack surface with the theoretical values from Irwin's formula [2]. This extrapolation technique is illustrated in Figure 1. The SIF results are calculated at two locations remote from the crack tip using equations (1) and (2). These results are then extrapolated to the crack tip using equation (3). This method can be used for computing Modes I, II



$$K_{I_A} = \frac{2\mu}{\kappa+1} \sqrt{\frac{2\pi}{r_A}} (\delta_{A_1} - \delta_{A_2}) \quad (1)$$

$$K_{I_B} = \frac{2\mu}{\kappa+1} \sqrt{\frac{2\pi}{r_B}} (\delta_{B_1} - \delta_{B_2}) \quad (2)$$

$$K_I = 2K_{I_A} - K_{I_B} \quad (3)$$

Figure 1. Schematic and equations illustrating implementation of displacement extrapolation technique used to compute stress intensity factors.

and III stress intensity factors for edge and embedded cracks.

## 2.4 Numerical Simulation of Crack Growth

Numerical simulation of crack growth provides a powerful predictive tool to use during the design phase as well as for evaluating the behavior of existing cracks. These simulations can be used to compliment experimental results and allow engineers to economically evaluate a large number of damage scenarios. Numerical methods are the most efficient way to simulate fatigue crack growth because crack growth is an incremental process where SIF values are needed at each increment as input to crack growth equations.

The boundary element method offers several advantages in crack growth simulation because high stress gradients at the crack front can be accurately modeled and the continuous re-meshing required to simulate crack growth is efficiently handled. The crack growth algorithm incorporated in the computer code allows the crack front to propagate as long as the effective SIF ( $K_{eff}$ ) is between the lower bound of the threshold SIF ( $K_{th}$ ) and the upper bound of the critical SIF ( $K_c$ ). These bounding limits in the crack growth algorithm restrict the analysis to stable crack growth and subcritical crack growth.

In order to simulate mixed-mode crack growth an incremental type analysis is used where knowledge of both the direction and size of the crack increment extension are necessary. For each increment of crack extension, a stress analysis is performed using the DBEM, and the SIF are evaluated. The incremental direction and size along the crack front for the next extension are determined by fracture mechanics criteria involving SIF as the prime parameters. The crack front is re-meshed and the next stress analysis is carried out for the new configuration. The computational cycle used to simulate crack growth is illustrated in the flowchart shown in Figure 2.

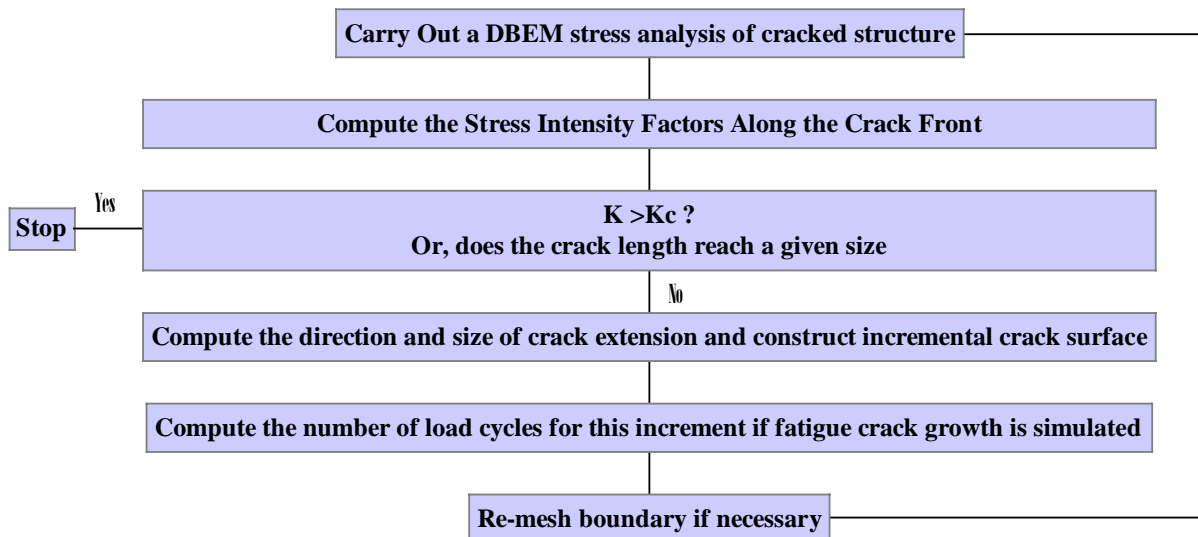


Figure 2. Computational cycle for numerical simulation of crack growth.

#### 2.4.1 Incremental Direction Growth Criteria

Several criteria have been proposed to describe the direction of crack propagation for mixed mode crack growth [3]. Only the minimum strain energy density criterion is discussed in this paper. The strain energy density criterion is based on the postulate that the direction of crack propagation at any point along the crack front is toward the region where the strain energy density factor is a minimum. The strain energy density factor is shown in equation (4).

$$S(\theta) = a_{11}K_I^2 + 2 a_{12}K_I K_{II} + a_{22}K_{II}^2 + a_{33}K_{III}^2 \quad (4)$$

The direction of crack growth is determined by minimizing this equation with respect to the angle theta ( $\theta$ ). The crack growth direction angle in the local coordinate plane perpendicular to the crack front can then be determined for each point along the crack front.

#### 2.4.2 Incremental Crack Extension Distance

The maximum incremental distance that a crack would be expected to propagate can be determined using the strain energy density criterion or empirical methods. This paper discusses an empirical method based on experimental fatigue crack growth data. A method based on actual material behavior may better approximate crack propagation in engineering materials. The combined use of equations (5), (6), (7) and (8) illustrate the use of the Paris fatigue growth crack equation for determining both the maximum crack extension distance and the incremental crack extension distances for all the neighboring points along the crack front. A similar method could be adopted using the NASGRO 2.0 equation.

$$K_{eff} = \sqrt{(K_I + |K_{III}|)^2 + 2K_{II}^2} \quad (5)$$

$$\frac{da}{dN} = C (\Delta K_{eff})^m \quad (6)$$

$$\Delta N = \frac{\Delta a_{max}}{(da/dN)_{max}} \quad (7)$$

$$\Delta a = \Delta N \frac{da}{dN} \quad (8)$$

The steps used to calculate the incremental crack extension distance are described below and intended to compliment the flowchart shown in Figure 2.

1. Conduct a stress analysis of the cracked structure using the DBEM.
2. Calculate  $\Delta K_{eff}$  for each point along the crack front using equation (5).
3. Use a fatigue crack growth relationship (Paris or NASGRO 2.0) to calculate crack growth rate ( $da/dN$ ) at each point along the crack front.
4. Determine the maximum value of  $da/dN$  along the crack front.
5. The maximum incremental crack distance ( $\Delta a_{max}$ ) is a fixed value based on initial crack front element dimensions. ( $\Delta a_{max}$  is taken where  $\Delta K_{eff}$  is a maximum and is equal to the length of the element side oriented perpendicular to the crack front).

6. Compute the number of cycles required to propagate the crack one increment using equation (7).
7. Scale the neighboring incremental crack extension distances along the crack front using equation (8).

### 3.0 APPLICATION IN THE AEROSPACE INDUSTRY

In order to demonstrate the accuracy and efficiency of the methodology discussed in the preceding sections two crack growth applications are described. The first application describes fatigue crack growth in a gear tooth and the second illustrates the use of the boundary element methodology to simulate repair of a cracked fuselage skin.

#### 3.1 Fatigue Crack Growth in a Titanium Gear Tooth

The growth of a crack from the root of a gear tooth was simulated to determine the safe operating life of the component. The boundary element model of the gear tooth is shown in Figure 3. An embedded semi-circular crack was located near the root of the gear tooth. The crack was oriented normal to the surface of the root

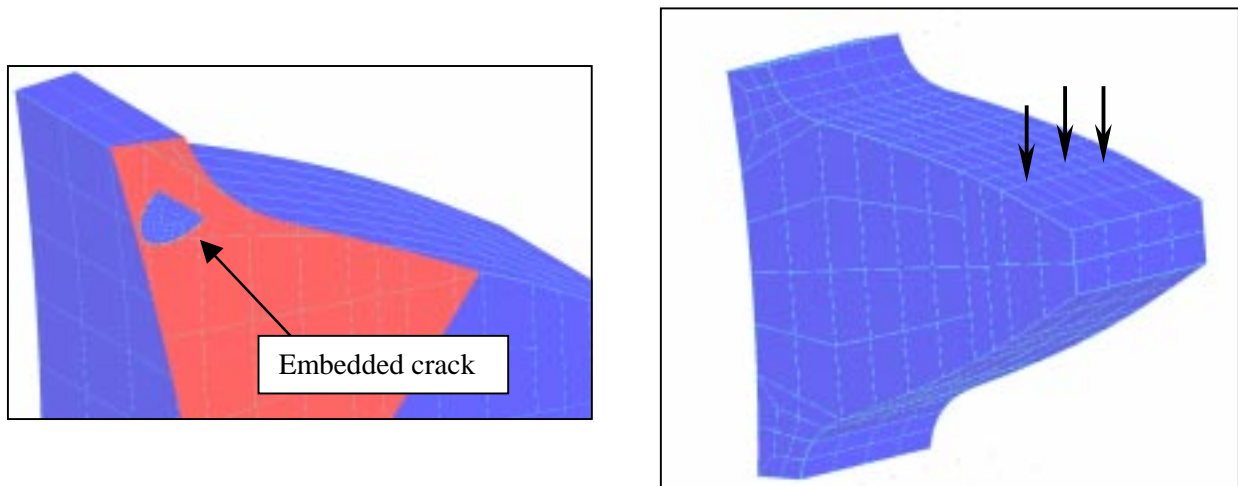


Figure 3. Boundary element model of titanium gear tooth. Embedded semi-circular crack shown located near root of gear tooth.

The gear tooth was made of titanium and material constants were elastic modulus  $E = 16,500$  ksi and Poisson's ratio  $\nu = 0.33$ . The fatigue crack growth curve fitting parameters were taken from the NASGRO 2.0 database where the material code P1CA13WA1 was selected. The gear tooth was loaded with uniform stress acting in a direction normal to the tooth surface. The load was applied near the end of the gear tooth in order to generate a tensile stress at the root. The fatigue crack analysis was conducted using constant amplitude cyclic loading with the stress ratio ( $R$ ) equal to zero.

The fatigue crack growth analysis was conducted by using the minimum strain energy density criterion to determine incremental crack growth direction. The incremental crack propagation distance was determined using the relationship between crack size increment and number of cycles defined in the NASGRO 2.0 equation. The effective stress intensity factor ( $K_{eff}$ ) was used in place of the maximum

stress intensity factor ( $K_{max}$ ) in the NASGRO 2.0 equation. The formulation of  $K_{eff}$  is discussed in detail in references [3, 4].

Fatigue crack growth was simulated using two incremental steps. The initial crack front and the crack growth path for the semi-circular crack are shown in Figure 4. The deformed shape of the crack surface is indicative of mixed mode crack growth. The variation in the crack growth rate along the crack front for the two crack increment steps is shown in Figure 5. A large increase in the crack growth rate is observed at the edge of the crack (locations A and A' in Figure 4).

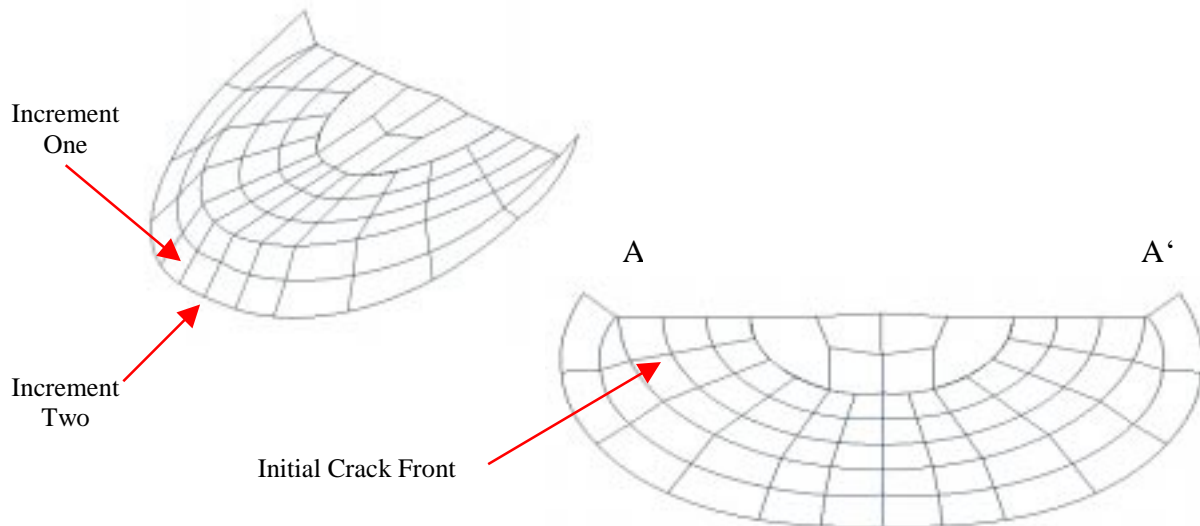


Figure 4. Two view of boundary element mesh showing deformed crack surface. Note “cupping” of crack which is typical for embedded crack subject to mixed mode loading.

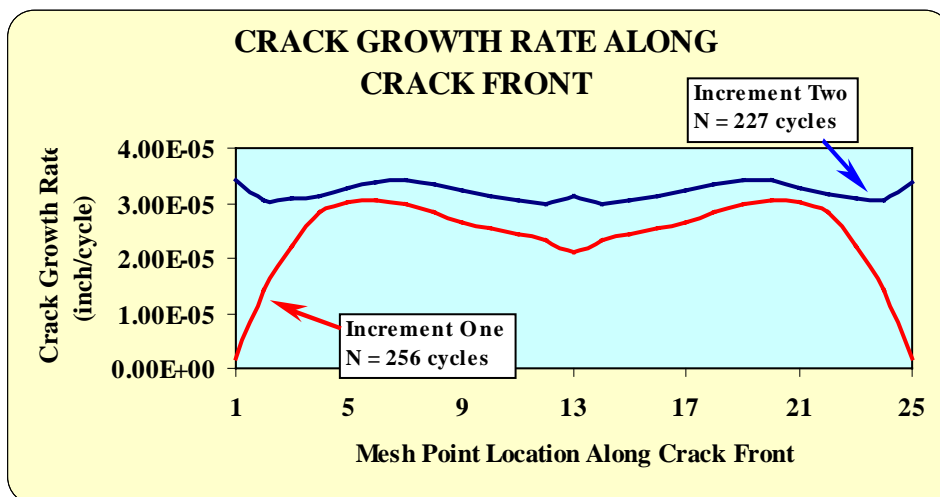


Figure 5. Plot of crack growth rate ( $da/dN$ ) along crack front.

Figures 6 and 7 show Mode I and Mode II SIF values along the crack front. These plots suggest the cracked behavior of the gear tooth is governed primarily by Mode I crack growth which is consistent with the loading and geometry. The  $K_I$  value is also observed to become more uniform along the crack front as the crack propagates. The  $K_{II}$  value approaches zero along the center section of the crack front but tends to increase toward the outer edges of the crack front (location A and A' shown in Figure 4). This suggests that there is an increasing component of shear stress acting at the edges of the crack. The  $K_{eff}$  reached a maximum value of 25.1 ksi  $\sqrt{\text{in}}$  during the second increment. This is still well below  $K_c$  (50 ksi  $\sqrt{\text{in}}$ ) and indicates that the crack would most likely have continued to propagate in a stable manner if additional crack extension increments were used in the analysis.

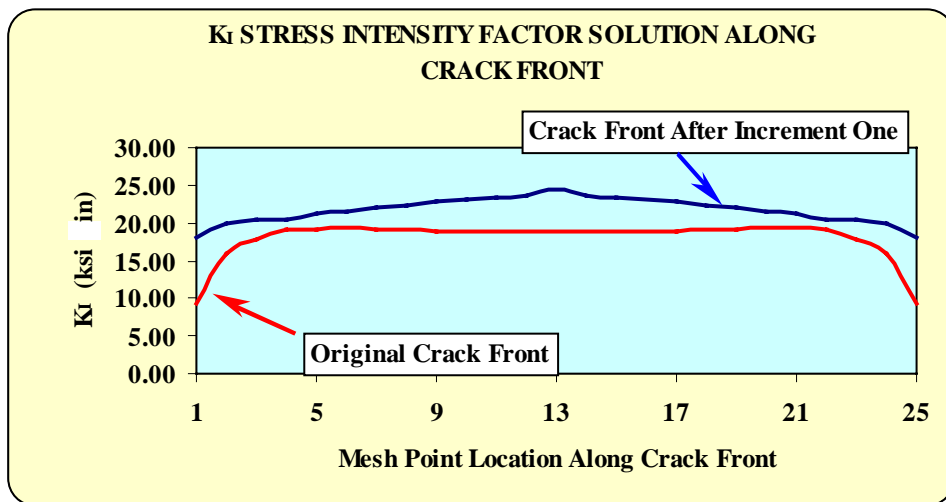


Figure 6. Plot of the Mode I stress intensity factor along the crack front at for the gear tooth model.

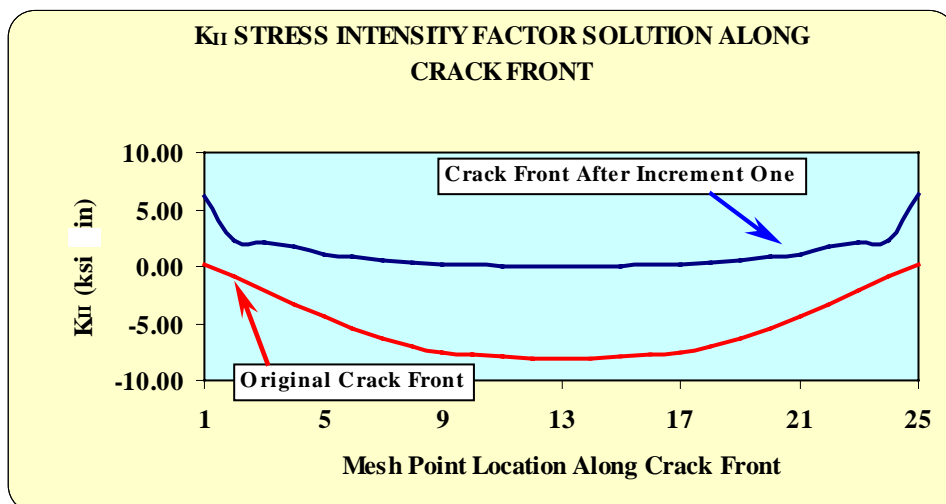


Figure 7. Plot of the Mode II stress intensity factor along the crack front at for the gear tooth model.

### 3.3 Simulation of a Patched Repair of a Cracked Fuselage Skin

The application discussed in the following section describes a simulated bonded patch repair of a crack in the stress-skin of an aircraft fuselage. This example is of interest given the recent endorsement of bonded repair techniques over some of the more common methods. The advantages of a bonded patch repair are that the creation of new damage near the repair site is less likely and the effectiveness of reducing crack growth is improved.

The first step in the analysis was to determine the SIF in a 0.0625-inch thick tension panel with a one-inch long center crack subject to a uniform tensile stress of 13,440 psi. The tensile panel was six inches wide by 15.6 inches long and made from 2024-T3 aluminum. The plate dimensions and loading were chosen so that the numerical results could be compared to experimental photoelastic work conducted by researchers in reference [5]. The numerical analysis produced a Mode I stress intensity factor of  $K_I = 18.2 \text{ ksi } \sqrt{\text{in}}$ . This value is within less than 1% of the value obtained from the experimental study and slightly greater than the theoretical value for the two-dimensional plane strain case.

The second step in the analysis involved testing the same tensile panel with a 2x3 inch rectangular patch added above the damage site (Figure 8). The patch was also made from 2024-T3 aluminum and had the same thickness as that of the tensile panel. The structural adhesive used to bond the patch to the tensile panel was represented as a zone interface with internal spring boundary conditions. Spring stiffness values, applied in the three global coordinate directions, were derived using the elastic properties of the structural adhesive and an assumed glue line thickness.

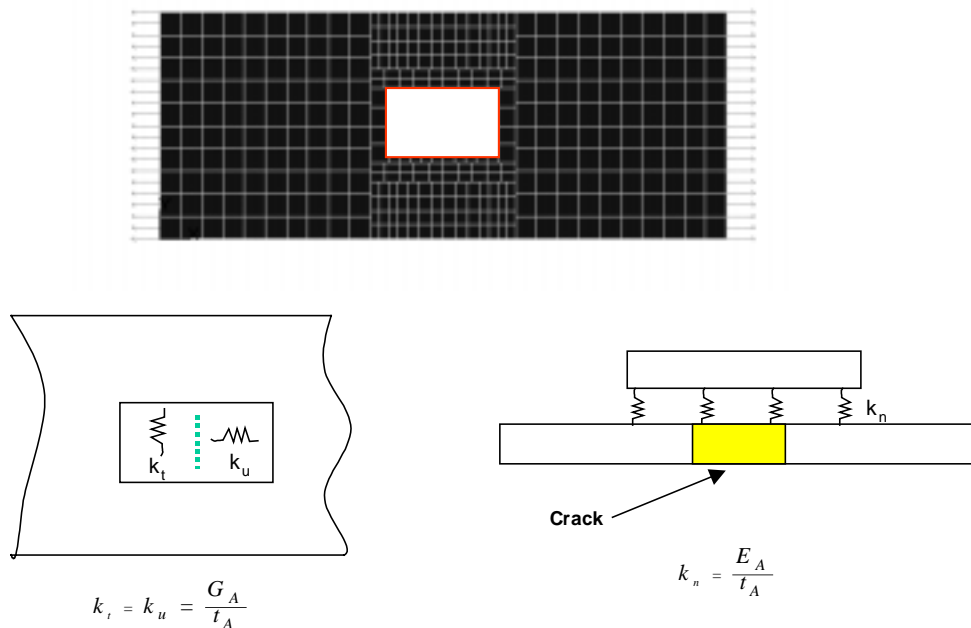


Figure 8. Boundary element model of aircraft skin with repair patch and schematic showing method to simulate structural adhesive properties ( $E_A = 560,000 \text{ psi}$ ,  $\nu = 0.4$ , bond thickness = 0.005 inch).

Numerical results obtained for the stress distribution in the patch, and the redistribution of stresses in the tension panel under the patch, agree very well with experimental results. An enlarged view of the patched area showing the stress redistribution is shown in Figure 9. Numerical results indicate that the patch reinforced the cracked region and carried load over the crack opening with a corresponding decrease in

stresses in the damaged region and in the SIF at the repaired crack tips. The reduced SIF values result in a corresponding decrease in the rate of crack growth.

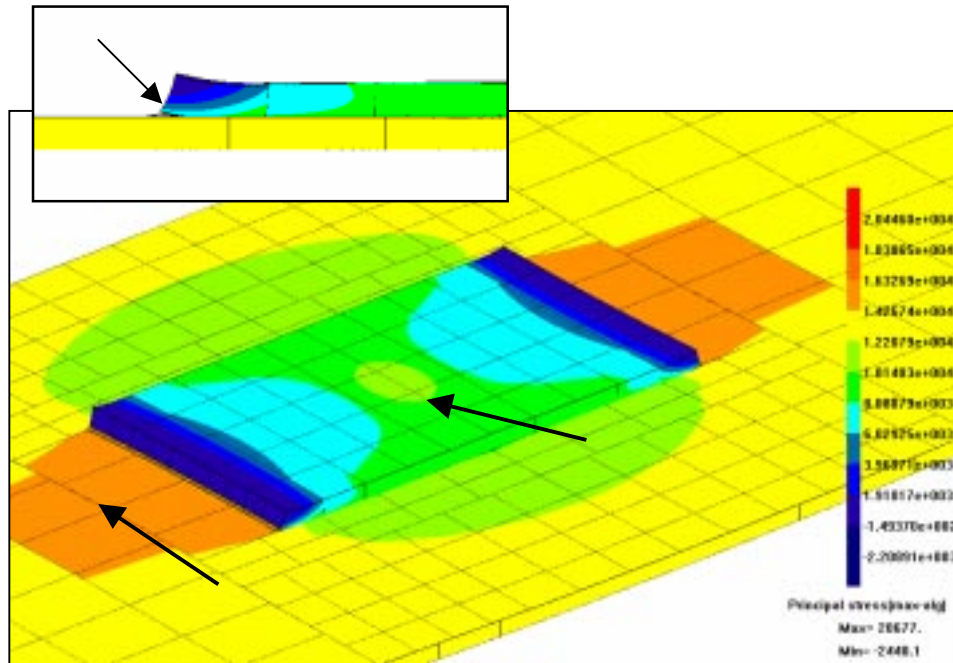


Figure 9. Principal stress results for patch repair simulation. Note stress transfer to plate and high tensile stress in patch above crack location. Also note “peeling” of patch edge.

The major difference between the numerical and experimental results was in the percent reduction in the SIF. The numerical model indicated a much greater reduction in the SIF. It is likely that this difference is a consequence of the method used to simulate the structural adhesive. It should also be noted that the experimental patch, although of similar dimensions, was elliptical in shape rather than rectangular and of slightly different material properties. These factors also limit the degree of comparison that can be made.

In order to investigate the sensitivity of  $K_I$  to the spring stiffness in the numerical model, a series of models were analyzed with varying spring stiffness. Better agreement with the results of the experimental model could be achieved as the spring stiffness was reduced from the initial values. In practice the numerical model would have to be calibrated using experimental results to better approximate the behavior of the adhesive before it could be used as an effective design tool.

No attempt was made to simulate the delamination observed, at higher loads, in the experimental model. However this behavior could be incorporated in the numerical model by adjusting the magnitude of the spring boundary conditions in the proper coordinate direction in accordance with the shear stress present at the patch/plate interface. Modeling of patch delamination would provide a more realistic understanding of the stress redistribution occurring in the repaired fuselage skin and facilitate assessment of the impact of the patch on arresting or reducing the crack growth rate.

## CONCLUSIONS

The boundary element method is a robust and efficient technology that can be used to investigate the impact of cracks on the performance of structural components. The accuracy of the method, in the field of fracture mechanics, is well documented in the technical literature. Two applications were discussed in this paper to demonstrate the effectiveness of a boundary element based computer code in evaluating the impact of fatigue crack growth on structural components. The first application described a fatigue crack growth analysis of a three-dimensional gear tooth with complex geometry and loading. The second application demonstrated that the computer code was effectively used to simulate the bonded patch repair of a cracked fuselage skin. This application also illustrates that aircraft repair simulation, when combined with appropriate experimental data, can provide engineers with an economical and powerful remedial design tool.

## REFERENCES

- [1] Portela, A., Aliabadi, M.H. and Rooke D.P., "Dual Boundary Element incremental analysis of crack propagation", *Int. Journal Computers and Structures*, Vol. 46, pp 237-247, (1993).
- [2] Aliabadi M.H. and Rooke D.P., *Numerical Fracture Mechanics*, Computational Mechanics Publications, Southampton UK / Boston MA, (1992).
- [3] Mi, Yaoming, *Three-Dimensional Analysis of Crack Growth*, Computational Mechanics Publications, Southampton UK / Boston MA, (1996).
- [4] Tanaka M. and Itoh, H., "New crack elements for boundary element analysis of elastostatics considering arbitrary stress singularities", *Applied Mathematical Modeling*, Vol. 11, 1987, p 357-363.
- [5] Hastie, R.L. Fredell, R., Dally, J.W., "A photoelastic study of crack repair", *Experimental Mechanics*, Vol. 38, No.1, March 1998, pp 29-36.
- [6] Hertzberg, R.W., *Deformation and Fracture Mechanics of Engineering Materials*, John Wiley & Sons, New York, New York, (1989).
- [7] Anderson, T.L. *Fracture Mechanics – Fundamentals and Applications*, CRC Press, Boca Raton, FL, (1995).
- [8] Cruse, T.A. and Meyers, G.J., "Three-Dimensional Fracture Mechanics Analysis", *Journal of the Structural Division*, ASCE, February 1977, pp 309-321.
- [9] Newman, J.C. and Raju, I.S., "Stress-Intensity Factor Equations for Cracks in Three-Dimensional Finite Bodies Subjected to Tension and Bending Loads", *NASA Technical Memorandum 85793*, April 1984, pp 1-38.
- [10] Brebbia, C.A., Telles, J.C.F. and Wrobel, L.C., *Boundary Element Techniques*, Springer-Verlag, Berlin, 1984.
- [11] Tada, H., Paris, P. and Irwin, G., *The Stress Analysis Cracks Handbook* (2<sup>nd</sup> edition), Paris Production Inc., St. Louis, Missouri, 1985.